



Enhanced magnetoelectric properties in $\text{Bi}_{0.95}\text{Ho}_{0.05}\text{FeO}_3$ polycrystalline ceramics

Poonam Uniyal^{a,b}, K.L. Yadav^{a,*}

^a Smart Material Research Laboratory, Department of Physics, Indian Institute of Technology, Roorkee 247667, India

^b School of Physics and Materials Science, Thapar University, Patiala 147004, India

ARTICLE INFO

Article history:

Received 10 February 2011

Received in revised form 30 August 2011

Accepted 2 September 2011

Available online 10 September 2011

Keywords:

Ceramics
Dielectric constant
Néel temperature
Magnetization
Multiferroic

ABSTRACT

Polycrystalline samples of Ho doped BiFeO_3 were prepared by solid state reaction method and effect of partial substitution of Ho on dielectric, magnetic and ferroelectric properties was studied. High temperature dielectric results show two dielectric anomalies both in ϵ and $\tan \delta$, out of which, anomaly at higher temperature ($\sim 400^\circ\text{C}$) could be ascribed to antiferromagnetic Néel temperature which, is a signature of magnetoelectric coupling. The magnetic moment is greatly improved and the maximum magnetization was found to be 0.736 emu/g . Saturated ferroelectric hysteresis loops were observed for $\text{Bi}_{0.95}\text{Ho}_{0.05}\text{FeO}_3$ with remnant polarization (P_r) = $1.59\ \mu\text{C/cm}^2$, maximum polarization (P_{max}) = $2.56\ \mu\text{C/cm}^2$ and coercivity (E_c) = $5.45\ \text{kV/cm}$. We have conducted comprehensive magnetoelectric and magnetodielectric properties at room temperature. Magnetic field induced ferroelectric hysteresis loop observed in $\text{Bi}_{0.95}\text{Ho}_{0.05}\text{FeO}_3$ is of prime importance.

© 2011 Elsevier B.V. All rights reserved.

1. Introduction

The rapid emergence of the field of spintronics, which followed the discovery of Giant Magnetoresistance, the last decade led to the study of new materials with potential applications in magneto-electronics [1,2]. Multiferroics is class of materials which combine several ferroic orders like ferromagnetism, ferroelectricity, ferroelasticity, etc. In absence of naturally occurring multiferroic materials, the current research activities of multiferroics are limited to few representative perovskite oxides, namely, BiFeO_3 , BiMnO_3 , etc., which combine several useful properties in the same material to device new functionalities in information storage, spintronics, etc. The large difference between magnetic and ferroelectric temperatures is one of the obstacles to the exploitation of multiferroics for real applications at room temperature. Bismuth ferrite shows room temperature magnetic ordering and ferroelectric ordering with antiferromagnetic Néel temperature (T_N) of 370°C and ferroelectric temperature (T_C) of 810°C [3,4]. Its crystal structure is described by the rhombohedral space group $R3c$ with no inversion center. This material shows promise for applications in sensor devices, memory devices and spintronics [5]. However, there are some drawbacks with BiFeO_3 for room temperature applications, such as high leakage current, high dielectric loss and weak antiferromagnetic character. The magnetoelectric interactions in the bulk samples of pure BiFeO_3 are weak because the main antiferromag-

netic G-type structure is modulated by a cycloid with a large period of $620\ \text{\AA}$ [6]. In this phase, the linear magnetoelectric effect is forbidden, while the much weaker quadratic magnetoelectric effect is allowed [7]. To implement the linear magnetoelectric interaction, the incommensurate magnetic structure should be destroyed. Chemical substitution could tune the incommensurate magnetic structure [8–13]. Various dopings have been studied so far and a general observation is that the radius of the A-site doping ion plays an important role in modifying the crystal structure, on which the resultant magnetism and ferroelectricity of the ceramic is dependent [14–16]. In general, isovalent substitution with a larger cation on the A site or a smaller cation on the B site would increase the stability of BiFeO_3 with respect to the binary oxides and possibly also with respect to the $\text{Bi}_2\text{Fe}_4\text{O}_9$ mullite and $\text{Bi}_{25}\text{FeO}_{39}$ sillenite phase [17]. Lanthanide ions are smaller than Bi^{3+} ions and are more basic, hence perovskite phase is obtained up to 15–20% substitution. Amirov et al. have reported enhancement in magnetic and magnetodielectric properties with a small substitution of lanthanum for bismuth in BiFeO_3 [15]. We present the results of electric and magnetic investigations of small substitution of Ho^{3+} for Bi^{3+} in Bismuth ferrite. In this letter, our aim was twofold, to study the multiferroic properties and to see if the material prepared is magnetoelectric at room temperature or not.

2. Experimental details

BiFeO_3 and $\text{Bi}_{0.95}\text{Ho}_{0.05}\text{FeO}_3$ ceramics were prepared by conventional solid state reaction method. Stoichiometric amounts of Bi_2O_3 , Ho_2O_3 and Fe_2O_3 were weighed and subsequently mixed in agate mortar for 4 h. The mixture was further calcined at 800°C for

* Corresponding author. Tel.: +91 1332 285744; fax: +91 1332 273560.

E-mail addresses: klyadav35@yahoo.com, uniyalpoonam@gmail.com (K.L. Yadav).

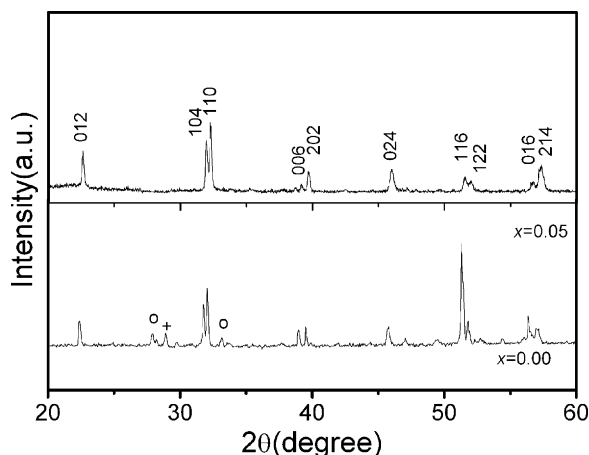


Fig. 1. The XRD pattern of BiFeO_3 (BFO) and $\text{Bi}_{0.95}\text{Ho}_{0.05}\text{FeO}_3$ (BHFO-5) samples, (o) and (+) represents the impurity phases $\text{Bi}_2\text{Fe}_4\text{O}_9$, $\text{Bi}_{36}\text{Fe}_{24}\text{O}_{57}$ respectively.

2 h in air. Phase identification was performed with an X-ray diffractometer using $\text{Cu K}\alpha$ radiation. Magnetization data were collected using Superconducting Quantum Interference Device (SQUID). The polarization–electric field (P–E) hysteresis loops were measured at room temperature by the modified Sawyer–Tower circuit (automatic P–E loop tracer system, Marine India Electr. Pvt. Ltd.). The dielectric measurements were done using an automated HIOKI 3532–50 Hi Tester, LCR meter capacitance. To study the magnetocapacitance measurement, Wayne Kerr 6500 high frequency LCR meter is used along with a magnet up to 12 kOe and having accuracy of 10 Oe (provided by Marine India Electr. Pvt. Ltd.).

3. Results and discussion

Fig. 1 shows the XRD patterns of pure BiFeO_3 (BFO) and $\text{Bi}_{0.95}\text{Ho}_{0.05}\text{FeO}_3$ (BHFO-5) samples. While majority of the diffraction peaks come from rhombohedral perovskite structure, there are small peaks of $\text{Bi}_2\text{Fe}_4\text{O}_9$ and $\text{Bi}_{36}\text{Fe}_{24}\text{O}_{57}$ in undoped BFO samples. These impurities are usually obtained along with BiFeO_3 , since BiFeO_3 is metastable with respect to $\text{Bi}_2\text{Fe}_4\text{O}_9$ (mullite phase) and $\text{Bi}_{25}\text{FeO}_{39}$ (sillenite phase) for $720 < T < 1040 \text{ K}$ [15]. These impurity peaks are nearly absent in BHFO-5 samples. Here Ho_2O_3 (a third component as a minor additive) in the solid solution accelerate the formation of BiFeO_3 . The lattice parameters for BFO are as follows; $a = 5.5746 \text{ \AA}$ and $c = 13.9831 \text{ \AA}$. These parameters are reduced to $a = 5.5654 \text{ \AA}$ and $c = 13.8761 \text{ \AA}$ for BHFO-5 samples in accordance with the ionic radii of Bi^{3+} (1.17 Å) and Ho^{3+} (1.015 Å) ions.

Fig. 2 shows dielectric constant (ϵ) and loss factor ($\tan \delta$) as a function of temperature for BFO and BHFO-5 samples. In BFO, dielectric constant shows a small peak at 200°C , and then there is monotonic increase near 370°C (**Fig. 2(a)**). The dielectric loss also shows a prominent peak around 200°C and then it increases beyond the value 10. This peak at 200°C could be attributed to transient interaction between oxygen ion vacancies and the Fe^{3+} and Fe^{2+} redox [16–18]. Actually Bi^{3+} volatilize when the samples are sintered at high temperatures for longer durations. A charge imbalance is created and Fe^{3+} gets converted to Fe^{2+} , giving rise to oxygen vacancies in the final product because of charge compensation. These oxygen vacancies are responsible for the electrical conductivity. The very high value of ϵ of the order of 1000 even at room temperature is indicative of highly conducting nature. The effect of space charge polarization due to oxygen ion vacancies is always observed in the entire temperature range. However due to thermally activated process, there is appreciable increase in space charge polarization and conductivity in the material at higher tem-

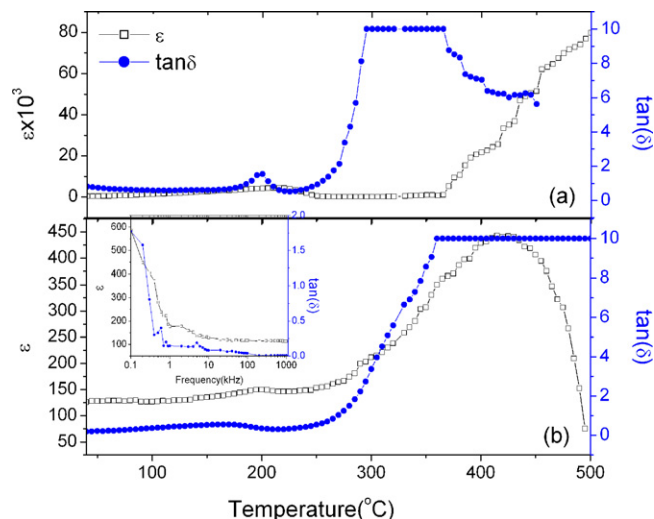


Fig. 2. The variation of dielectric constant (ϵ) and $\tan(\delta)$ with temperature of (a) BFO and (b) BHFO-5 respectively. Inset of (b) shows the frequency dependence of (ϵ) and $\tan(\delta)$ of BHFO-5 sample.

perature for which the ϵ and $\tan(\delta)$ values shoot up to very high value.

Fig. 2(b) clearly reflects a role of Ho in modifying dielectric behavior of BHFO-5. The replacement of some volatile Bi^{3+} with the non volatile Ho^{3+} may prevent oxygen ion vacancies causing stability of $\text{Fe}^{3+}/\text{Fe}^{2+}$ couple-oxygen vacancy interaction. Hence, the peak around 200°C which was prominent for BFO is highly reduced for BHFO-5, also the ϵ_{max} (ϵ corresponding to transition temperature) is 445 whereas the dielectric constant shows values of the order of 10^4 . This indicates that the oxygen ion vacancy in BHFO-5 is controlled by Ho doping and thereby the resistivity is improved.

There is a clear signature of antiferromagnetic transition temperature for Ho doped BHFO-5, the peaks in the permittivity patterns obtained here may be attributed to change from one state of electric dipole ordering to another because of antiferromagnetic transitions/possible magnetoelectric coupling effect.

According to Landau–Ginzburg theory, destruction of spin cycloid of BFO leads to enhanced ME interaction, which can improve both the effective magnetic susceptibility and the ferroelectric remnant polarization of multiferroics [19,20]. This may be explained by the equations, where polarization and magnetization are calculated as a derivative of free energy

$$P_i(\vec{E}, \vec{H}) = -\frac{\partial F}{\partial E_i} = P_i^S + \epsilon_0 \epsilon_{ij} E_j + \alpha_{ij} H_j + \frac{1}{2} \beta_{ijk} H_j H_k + \gamma_{ijk} H_i E_j - \dots \quad (1)$$

$$M_i(\vec{E}, \vec{H}) = -\frac{\partial F}{\partial H_i} = M_i^S + \mu_0 \mu_{ij} H_j + \alpha_{ij} E_j + \beta_{ijk} E_j H_k + \frac{1}{2} \gamma_{ijk} E_i E_j - \dots \quad (2)$$

where \vec{P}^s and \vec{M}^s denote the spontaneous polarization and magnetization, whereas $\hat{\epsilon}$ and $\hat{\mu}$ are the electric and magnetic susceptibilities [21]. The tensor $\hat{\alpha}$ corresponds to induction of polarization by a magnetic field or of magnetization by an electric field which is designated as the linear ME effect and higher-order ME effects terms are parameterized by the tensors $\hat{\beta}$ and $\hat{\gamma}$ respectively. Disappearance of antiferromagnetic order can have strong impact on ferroelectric order through α_{ij} and/or β_{ijk}/γ_{ijk} near antiferromagnetic transition resulting in dielectric anomalies, i.e., ME coupling. When either the canting angle of canted antiferromagnetic order decreases to zero or the space-modulated spin structure disappears at temperatures below antiferromagnetic transition temperature,

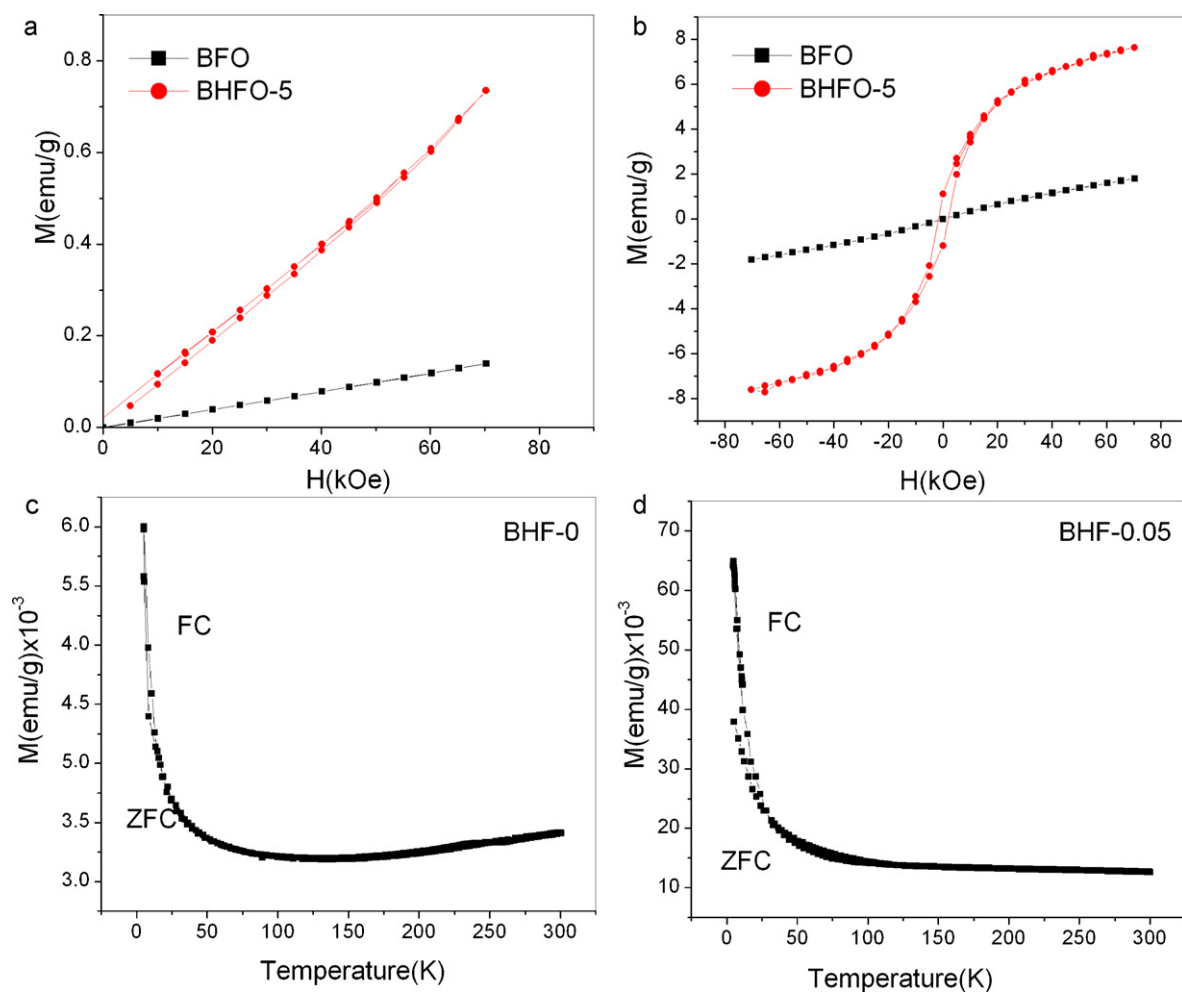


Fig. 3. Field dependence of magnetization of BFO and modified BHFO-5 at 300 K and 5 K are shown by (a) and (b) respectively. Variation of magnetization (ZFC and FC) with temperature BFO and modified BHFO-5 are shown in (c) and (d) respectively.

the vibration of antiferromagnetic order can also impact ferroelectric order.

The frequency dispersion of ϵ and $\tan(\delta)$ for BHFO-5 samples is shown in the inset of Fig. 2(b). Initial decrease in ϵ and $\tan(\delta)$ with frequency (up to 100 kHz) can be explained by the phenomenon of dipole relaxation wherein at low frequencies the defects related dipoles are able to follow the frequency of the applied field providing high values of ϵ , but begin to lag behind the field with increasing frequency.

Room-temperature measurements of the magnetization of BFO and BHFO-5 samples as a function of the applied magnetic field are shown in Fig. 3(a). As in the case of pure BFO, the $M(H)$ dependence of Ho^{3+} substituted compound shows a linear character without any spontaneous magnetization, thus confirms the antiferromagnetic nature of the samples. BiFeO_3 is known to be antiferromagnetic with a G type magnetic structure but has a residual magnetic moment due to a canted spin structure. The magnetic moment of the samples is greatly improved with increasing Ho doping content in BiFeO_3 . For example, the magnetic moment of BFO measured at 70 kOe is 0.141 emu/g at room temperature, while the value is 0.736 emu/g for BHFO-5. The magnetic hysteresis loop for BHFO system at 5 K is shown in Fig. 3(b). The loop obtained was fully saturated at 5 K. Impurities such as $\gamma\text{Fe}_2\text{O}_3$ are reported to contribute towards magnetization whereas $\text{Bi}_2\text{Fe}_4\text{O}_9$ is paramagnetic at room temperature and undergoes a transition to an antiferromagnetic state at 264 K. Since no $\gamma\text{Fe}_2\text{O}_3$ exist in the ceramics, the enhanced magnetization is believed to be intrinsic. The cycloid spin structure

in pure BiFeO_3 , which hinders the observation of any linear magnetoelectric effect is supposed to be suppressed by lanthanide ion dopings [15,22]. We believe that Ho doping in BHFO-5 releases the latent magnetization locked within this structure, and enhances the magnetic moment.

The zero field cooled (ZFC) magnetization was obtained during sample heating after cooling from 300 K in zero field, while the field cooled (FC) magnetization was measured during heating after cooling in a magnetic field. The results (shown in Fig. 3(c) and (d)) reveal a decrease in magnetization down to 120 K and then a steep increase is observed. This steep rise in magnetization value of BFO suggests the presence of uncompensated antiferromagnetic spins.

A comparison of P–E loops with and without magnetic fields is shown in Fig. 4(a–d) at various applied alternating fields. We have obtained saturated P–E loops with remnant polarization (P_r) = 1.88 $\mu\text{C}/\text{cm}^2$, maximum polarization (P_{max}) = 2.96 $\mu\text{C}/\text{cm}^2$ and coercivity (E_c) = 5.45 kV/cm. The observed P–E loops are 10 times bigger than reported in other bulk Bismuth ferrite samples [18,23] and is comparable to some doped Bismuth ferrite thin films [24–28]. It is clear from the Fig. 4(a–e) that the remnant polarization is decreased on the application of high frequency field in absence of magnetic field. At all the frequencies, remnant polarization was found to increase in the presence of magnetic field. In ferroelectric materials, the space charge polarization effect is dominant at high temperatures and low frequencies. Had it been the effect of space charge only, the enhancement of polarization with the external magnetic field should be highly suppressed at

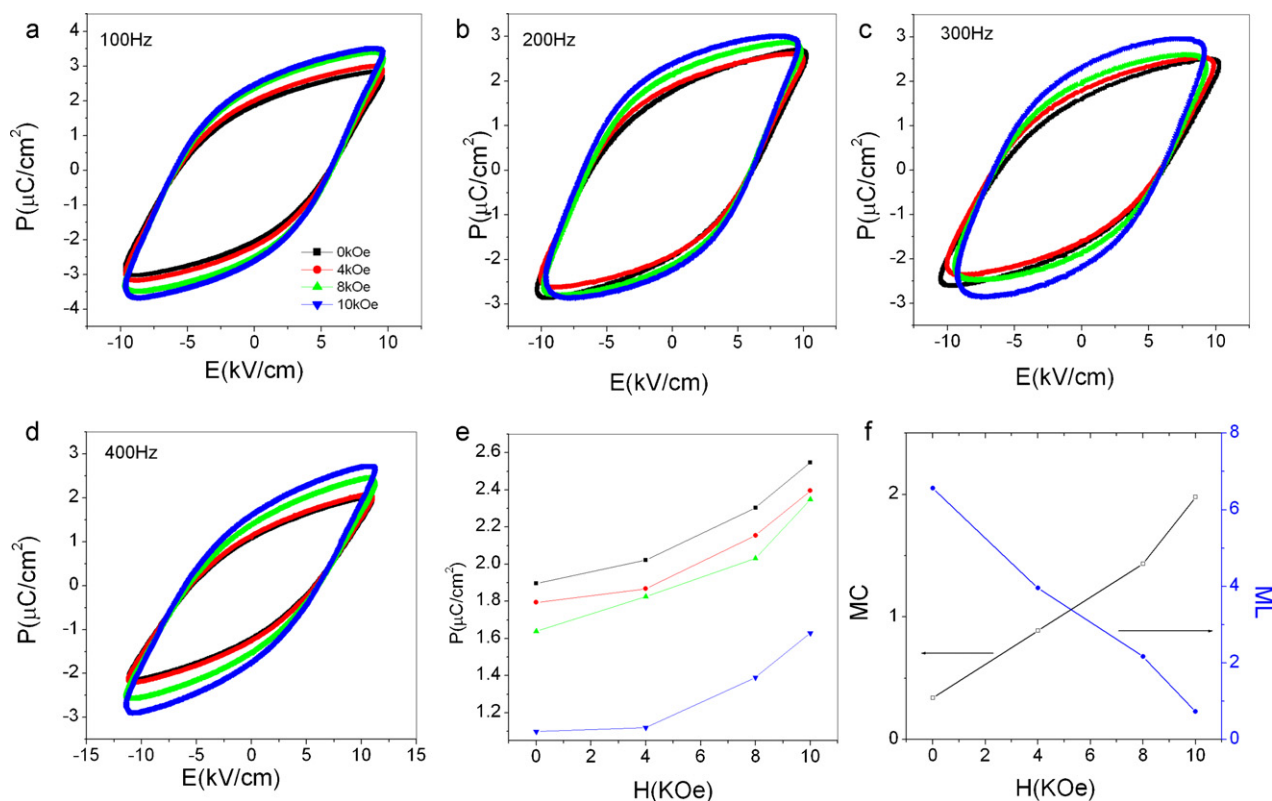


Fig. 4. (a–d) The room temperature P–E loops for $\text{Bi}_{0.95}\text{Ho}_{0.05}\text{FeO}_3$ (BHFO-5) sample at various applied magnetic fields for alternating fields of 100–400 Hz. (e) The variation of remnant polarization with applied magnetic field at various frequencies and (f) shows the percentage change in dielectric constant and dielectric loss respectively for $\text{Bi}_{0.95}\text{Ho}_{0.05}\text{FeO}_3$ (BHFO-5) sample.

400 Hz. But it is not the case and we observed increase in remnant polarization with the increase in magnetic field for the sample at all the frequencies. This observation clearly suggests that the sample shows magnetoelectric effect and it is an intrinsic property of the material and not the space charge effect. The variation of P_r with the applied magnetic field is shown in Fig. 4(e). With increase in magnetic field from 0 Oe to 10 kOe the P_r values increase continuously from $1.88 \mu\text{C}/\text{cm}^2$ to $2.59 \mu\text{C}/\text{cm}^2$. We have also measured the magnetocapacitance by directly measuring the capacitance as a function of magnetic field. The data gives a linear magnetic field dependence. We measured capacitance and dielectric loss at a frequency of 1 kHz as a function of magnetic field ranging from 0 Oe to 10 kOe. The magnetocapacitance measurements are shown in Fig. 4(f).

The magnetocapacitance is defined as

$$MC = \frac{\varepsilon'(H) - \varepsilon'(0)}{\varepsilon'(0)} \times 100 \quad (3)$$

and the magnetolosses, defined as

$$ML = \frac{\tan \delta(H) - \tan \delta(0)}{\tan \delta(0)} \times 100 \quad (4)$$

The increase in dielectric constant along with a decrease in dielectric loss on the application of magnetic field also supports the fact that magnetic field is not affecting the conduction charge; otherwise the loss should have also been increased. BiFeO_3 is assumed to have a spin canted structure. When a magnetic field is applied, it helps the recanting of the spin by facilitating the antiferromagnetic domain switching in such a way that the activation energy for the switching of the electrical polarization domains is reduced. As a result, the electrical polarization that could be switched by an electric field is varied by a magnetic field.

4. Conclusions

In conclusion, we have been successful in synthesizing a new multiferroic compound ($\text{Bi}_{0.95}\text{Ho}_{0.05}\text{FeO}_3$) by conventional solid state reaction method. We have studied the effect of Holmium doping on dielectric, magnetic and ferroelectric properties of BFO compound at room temperature. Even a small amount of doping has led to enhancement of multiferroic properties. The magnetic field dependence of remnant polarization, dielectric constant and dielectric loss shows that the system is a magnetoelectric as well as magnetodielectric material at room temperature. Hence thin films of this material could find use in device application.

Acknowledgements

P. Uniyal would like to thank AICTE for the financial support in the form of National Doctoral Fellowship.

References

- [1] N.A. Spaldin, S.W. Cheong, R. Ramesh, *Phys. Today* 63 (2010) 38–43.
- [2] W. Chen, S. Shannigrahi, X.F. Chen, Z.H. Wang, W. Zhu, O.K. Tana, *Solid State Commun.* 150 (2010) 271–274.
- [3] I. Sosnowska, R. Prezenioslo, P. Fischer, V.A. Murashov, *J. Magn. Magn. Mater.* 160 (1996) 384–385.
- [4] J.B. Neaton, C. Ederer, U.V. Whgmare, N.A. Splaldin, K.M. Rabe, *Phys. Rev. B* 71 (2005) 014113–14118.
- [5] Z.X. Cheng, X.L. Wang, K. Ozawa, H. Kimura, *Appl. Phys. Lett.* 40 (2007) 703–713.
- [6] Yuan-Hua Lin, Qinghui Jiang, Yao Wang, Ce-Wen Nan, Lin Chen, Jian Yu, *Appl. Phys. Lett.* 90 (2007) 172507–172513.
- [7] Z.X. Cheng, X.L. Wang, S.X. Dou, H. Kimura, K. Ozawa, *J. Appl. Phys.* 104 (2008) 116109–116113.
- [8] V.S. Puli, A. Kumar, N. Panwar, I.C. Panwar, R.S. Katiyar, *J. Alloys Compd.* 509 (2011) 8223–8227.
- [9] P. Uniyal, K.L. Yadav, *Mater. Lett.* 62 (2008) 2858–2861.
- [10] P. Uniyal, K.L. Yadav, *J. Appl. Phys.* 105 (2009) 07D914-3.

- [11] D. Varshney, A. Kumar, K. Verma, *J. Alloys Compd.* 509 (2011) 8421–8426.
- [12] V.A. Khomchenko, D.A. Kiselev, J.M. Vieira, A.L. Kholkin, M.A. Sîa, Y.G. Pogorelov, *Appl. Phys. Lett.* 90 (2007) 242901–242903.
- [13] V.A. Khomchenko, D.A. Kiselev, J.M. Vieira, J. Li, A.L. Kholkin, A.M.L. Lopes, Y.G. Pogorelov, J.P. Araujo, M.J. Maglione, *Appl. Phys. Lett.* 103 (2008) 024105–24113.
- [14] A. Moure, J. Tartaj, C. Moure, *J. Alloys Compd.* 509 (2011) 7042–7046.
- [15] F. Azough, R. Freer, M. Thrall, R. Cernik, F. Tuna, D. Collison, *Eur. J. Ceram. Soc.* 30 (2010) 727–736.
- [16] M.S. Sverre, E. Mari-Ann, G. Tor, *Chem. Mater.* 21 (2009) 169–173.
- [17] A.A. Amirov, A.B. Batdalov, S.N. Kallaev, Z.M. Omarov, I.A. Verbenko, O.N. Razumovskaya, L.A. Reznichenko, L.A. Shilkina, *Phys. Solid State* 51 (2009) 1189–1192.
- [18] Z.X. Cheng, A.H. Li, X.L. Wang, S.X. Dou, K. Ozawa, H. Kimura, S.J. Zhang, T.R. Shrout, *J. Appl. Phys.* 103 (2008), 07E507–07E509.
- [19] S. Karimi, I.M. Reaney, I. Levin, I. Sterianou, *Appl. Phys. Lett.* 94 (2009) 112903–112905.
- [20] R.K. Mishra, Dillip K. Pradhan, R.N.P. Choudhary, A. Banerjee, *J. Phys. Condens. Mater.* 20 (2008) 045218–045225.
- [21] B. Ruetter, S. Zvyagin, A.P. Pyatakov, A.A. Bush, J.F. Li, V.I. Belotelov, A.K. Zvezdin, D. Viehland, *Phys. Rev. B* 69 (2004) 064114–064120.
- [22] N. Wang, J. Chen, A. Pyatakov, A.K. Zvezdin, J.F. Li, L.E. Cross, D. Viehland, *Phys. Rev. B* 72 (2005) 104434–104438.
- [23] M. Fiebig, *J. Phys. D* 38 (2005) R123–R152.
- [24] P. Uniyal, K.L. Yadav, *J. Phys.: Condens. Mater.* 21 (2009) 012205–012208.
- [25] F. Chang, N. Zhang, F. Yang, S. Wang, G. Song, *J. Phys. D: Appl. Phys.* 40 (2007) 7799–7803.
- [26] Z. Quan, W. Liu, H. Hu, S. Xu, B. Sebo, G. Fang, M. Li, X. Zhao, *J. Appl. Phys.* 104 (2008) 084106–084115.
- [27] P. Kharel, S. Talebi, B. Ramachandran, A. Dixit, V.M. Naik, M.B. Sahana, C. Sudhakar, R. Naik, M.S.R. Rao, G. Lawes, *J. Phys. Condens. Mater.* 21 (2009) 036001–036006.
- [28] Y. Wang, C.W. Nan, *J. Appl. Phys.* 103 (2008) 024103–024108.